The Astrophysical Journal, 833:94 (6pp), 2016 December 10 doi:10.3847/1538-4357/833/1/94

ON THE PRESENCE OF TWO POPULATIONS OF SUNSPOTS

Yury A. Nagovitsyn[1,3] and Alexei A. Pevtsov[2,4]
[1] Central (Pulkovo) Astronomical Observatory, Saint Petersburg, 196140, Russian Federation; nag@gao.spb.ru
[2] National Solar Observatory, Boulder, CO 80303, USA; apevtsov@nso.edu
Received 2016 May 18; revised 2016 September 26; accepted 2016 October 7; published 2016 December 9

ABSTRACT

Using historical (1894–1976) and more modern (1977–2014) observations, we investigate statistical properties of distributions of sunspot areas and their long-term variations. We confirm the presence of two populations of sunspots with smaller and larger areas, and show that sunspot/group lifetime can be used to separate the two populations on small short-lived sunspot groups (SSG) and large long-lived groups (LLG). The area properties of LLG are nearly constant over the entire period of observations, while the SSGs show significant long-term variations. Based on the presence of long-term variations in one component and the absence of those in the other, we suggest that the production of two populations of sunspots (SSG and LLG) may be affected by different processes.

Key words: Sun: activity – sunspots

1. INTRODUCTION

Several recent studies used the distribution of sunspots by their area to demonstrate the presence of two distinct populations of sunspots. Thus, for example, using observations from Kislovodsk Mountain Astronomical Station (KMAS), Nagovitsyn et al. (2012) showed that the distribution of sunspot areas can be represented by a combination of two log-normal components. Tlatov & Pevtsov (2014) described the presence of two components, which they classified as transitional and mature sunspots, in sunspot observations from the Helioseismic and Magnetic Imager on board the *Solar Dynamic Observatory*. Cho et al. (2015) showed that the distributions of umbral areas of transitional and mature sunspots have distinctly different properties. Based on the analysis of several historical data sets, Muñoz-Jaramillo et al. (2015) concluded that only large sunspots form a log-normal contribution; distribution of small sunspots follows a Weibull functional dependency. The latter was interpreted as signature of a fragmentation process, while the log-normal distribution of large sunspots is seen primarily as the contribution from growth and dynamo processes. Pevtsov et al. (2011) suggested that bimodal distribution of sunspots may be indicative of a distributed dynamo, with large sunspots forming deeper in the convection zone and small sunspots forming in more shallow layers. Indeed, the helioseismic observations indicate the presence of two areas of high gradient in solar rotation. One area is situated at the bottom of the convection zone (the so-called tachocline) and the other is in the upper convection zone, near the photosphere (the so-called leptocline, Godier & Rozelot 2001). Measurements of solar rotation using sunspots as tracers indicate the difference in rotation rates between large and small sunspots, with the latter group exhibiting rotation rates similar to the solar photosphere (Ward 1966; Howard 1984).

The relative contribution of small and large sunspots may vary from one cycle to the other (e.g., Lefèvre & Clette 2011). Nagovitsyn et al. (2012) demonstrated that such changes in the relative contribution (of small and large spots) may explain an apparent decline in the mean sunspot field strengths reported by Penn & Livingston (2006, 2011). On the other hand, the properties of distribution of large sunspots (when taken separately) could exhibit clear variations with the phase of solar cycle (as was observed by Pevtsov et al. 2011).

In this article, we continue exploring the signature of two distinct populations of sunspots. We employ a combined data set of sunspot areas from the Royal Greenwich Observatory (RGO) and KMAS, as described in Section 2. Based on the analysis of these data, we show that two populations differ not only in their size but in their lifetime (Section 3).

2. OBSERVATIONS

For this study, we use a combination of two data sets: the sunspot group area from the RGO, and the KMAS (www.solarstation.ru of the Central (Pulkovo) Astronomical Observatory. The RGO data set of daily photoheliographic observations starts in 1874 (Willis et al. 2013). During the period 1874–1885, the RGO observations were supplemented by photographs from Harvard College (USA), the Melbourne Observatory (Australia), Dehra Dûn (India), and the Royal Alfred Observatory (Mauritius) to fill many of the gaps in the early Greenwich series. From 1886–1909, the contributing stations were Greenwich, Dehra Dûn, Mauritius, and later, Kodaikanal). After 1910, the contributing observatories were Greenwich, the Royal Observatory at the Cape of Good Hope (South Africa), Dehra Dûn and the Kodaikanal Observatory in India, with some occasional data provided by the US Naval and the Mount Wilson observatories. In 1976, the RGO data set was terminated. In 1977, the US Air Force begun providing sunspot area data using the observations from its Solar Optical Observing Network (SOON). Although in the past, the (SOON) data set was often used as a continuation of the RGO data set of sunspot areas, it has a known deficiency in the measurements of smallest sunspots and pores (e.g., Muñoz-Jaramillo et al. 2015). On the other hand, the observations of sunspot areas from the KMAS, which start in 1954, are more uniform and include the smallest sunspots and pores comparable to the RGO sunspot size limit. By their cumulative distribution, KMAS group areas are similar to RGO data

[3] Saint Petersburg State University of Aerospace Instrumentation, Bolshaya Morskaya ul. 67, St. Petersburg, 190000 Russian Federation.
[4] ReSoLVE Centre of Excellence, Space Climate research unit, 90014 University of Oulu, Finland.

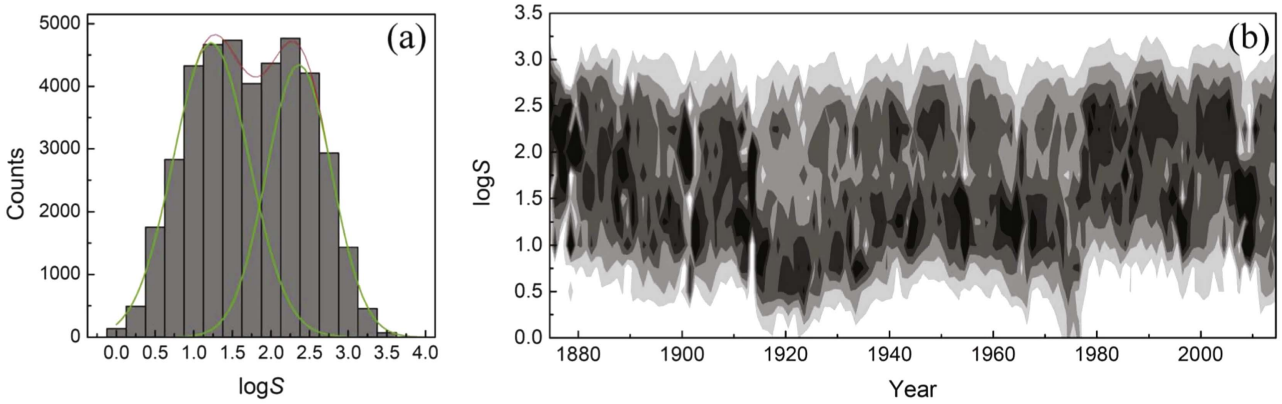

Figure 1. (a) Distribution of group areas (log S) from RGO data. Green lines show Gaussian functions fitted to two separate components of the distribution. The red line represents the sum of these fitted Gaussian functions. (b) 2D annualized probability density function (PDF) of combined RGO–KMAS (1874–2013) group areas. Outlined levels (from lighter to darker colors) correspond to five equidistant levels in distribution shown in panel (a).

(Muñoz-Jaramillo et al. 2015, who established a proportionality constant between RGO sunspot group areas and KMAS as 1.07 or 0.93 to convert from KMAS to RGO). Thus, for the period 1977–2014, we employ sunspot areas observed at KMAS (Tlatov et al. 2016).

3. TWO POPULATIONS OF SUNSPOT GROUPS

3.1. Group Areas

Sunspot groups are not static objects: as an active region develops its area increases and reaches a maximum within 2–3 days after its emergence (e.g., Pevtsov et al. 2003). According to a review article by van Driel-Gesztelyi & Green (2015), a lifetime of active regions with fully developed sunspots varies between weeks and months. The rise phase takes between 3% and 15% of a group's lifetime, which also translates to a few days from the beginning of the emergence of a group to the maximum of its development (maximum area). To take into account these evolutionary changes in group areas, for each group in the RGO–KMAS data set, we selected the largest area of this group. Since some groups will reach their maximum area on the side of the Sun not visible from Earth, one could expect a slight enhancement in small group areas. However, with a rapid growth phase of only a few days, we do not expect that such enhancement will have a significant effect on our conclusions. Figure 1(a) shows the distribution of $\log S$ (logarithm of group areas) for the combined RGO–KMAS data set. The distributions were constructed using an equal bin size of $\Delta = 0.25$ in the logarithm of group areas. The distribution is clearly bimodal, with one component peaking at about 16 M.S.H. (millionth of solar hemisphere, $\log S \approx 1.2$) and the other at about 316 M.S.H. ($\log S \approx 2.5$). The former corresponds to a round feature with 7.6 Mm in diameter (a pore or a rudimentary sunspot) and the latter is about 350 Mm in diameter, or about the size of a regular sunspot. To separate the two components, we fit the observed distributions by a combination of two Gaussian functions. The fitting was done with the help of the data analysis software package "ORIGIN," which uses the Levenberg–Marquardt algorithm to iteratively adjust the amplitude, mean, and standard deviation of each fitted Gaussian, until the best-fitted solution is found (e.g., Press et al. 1992). The fitted Gaussians are shown in Figure 1(a) as blue profiles, and their sum is shown as a red double-peaked profile.

The properties of distributions could be affected significantly by the binning process. To investigate the effects of binning, we constructed the distributions with the double (2Δ) and half ($\Delta/2$) of the original bin size ($\Delta = 0.25$). For each of these cases, we also shifted the origin of bins by half of the bin size. The distributions were fitted by a two-Gaussian model using the "ORIGIN" software package, as described earlier. The results of this exercise (see Figure 2) indicate that the bimodal distribution of sunspot areas is not significantly affected by a selection of bin size or the origin of the bins. Table 1 shows the mean and standard deviation of two Gaussian functions fitted to distributions in Figure 2. The means of the two fitted Gaussians do not overlap within one σ, and thus, are distinctly different. The correlation coefficients between fitted bimodal and observed distribution are very high (see r in Table 1), which further supports the use of bimodal fitting to the data. For this test, we used only RGO data.

As an additional test, let us consider a "null hypothesis" that the observed distribution of group areas could be represented by a single Gaussian distribution (i.e., that two normal distributions fitted to the observations are equal to each other). Then, a t-value of the Student's t distribution is (e.g., Gmurman 1968):

$$Z_{\rm obs} = \frac{x_{\rm L} - x_{\rm R}}{\sqrt{\sigma_{\rm L}/n + \sigma_{\rm R}/m}} \quad (1)$$

where x and σ are the mean and standard deviation of left (L) and right (R) Gaussians. m, n are the size of each distribution.

Using the Laplace probability distribution

$$\Phi(z_{\rm cr}) = (1 - \alpha)/2 \quad (2)$$

and significance level $\alpha = 0.01$, we find $z_{\rm cr} = 2.58$. The null hypothesis cannot be rejected if $Z_{\rm obs}$ is smaller than $z_{\rm cr}$. In our case, for six distributions shown in Figure 2 $Z_{\rm obs} = [246, 242, 254, 254, 255, 255] > z_{\rm cr}$, and thus, a null hypothesis that the distributions shown in Figures 1 and 2 could be represented by a single Gaussian can be rejected at 1% level.

The bi-modality in sunspot group distribution is present in different cycles and different phases of each cycle: a 2D annualized PDF (Figure 1(b)) shows two distinct bands in the distribution of group areas. In some cycles (e.g., cycle 15, 1913–1923; cycle 16, 1923–1933; cycle 20, 1964–1976), the "small area" component has larger amplitude than the "large area" component. Figure 3 shows bi-Gaussian fits to the

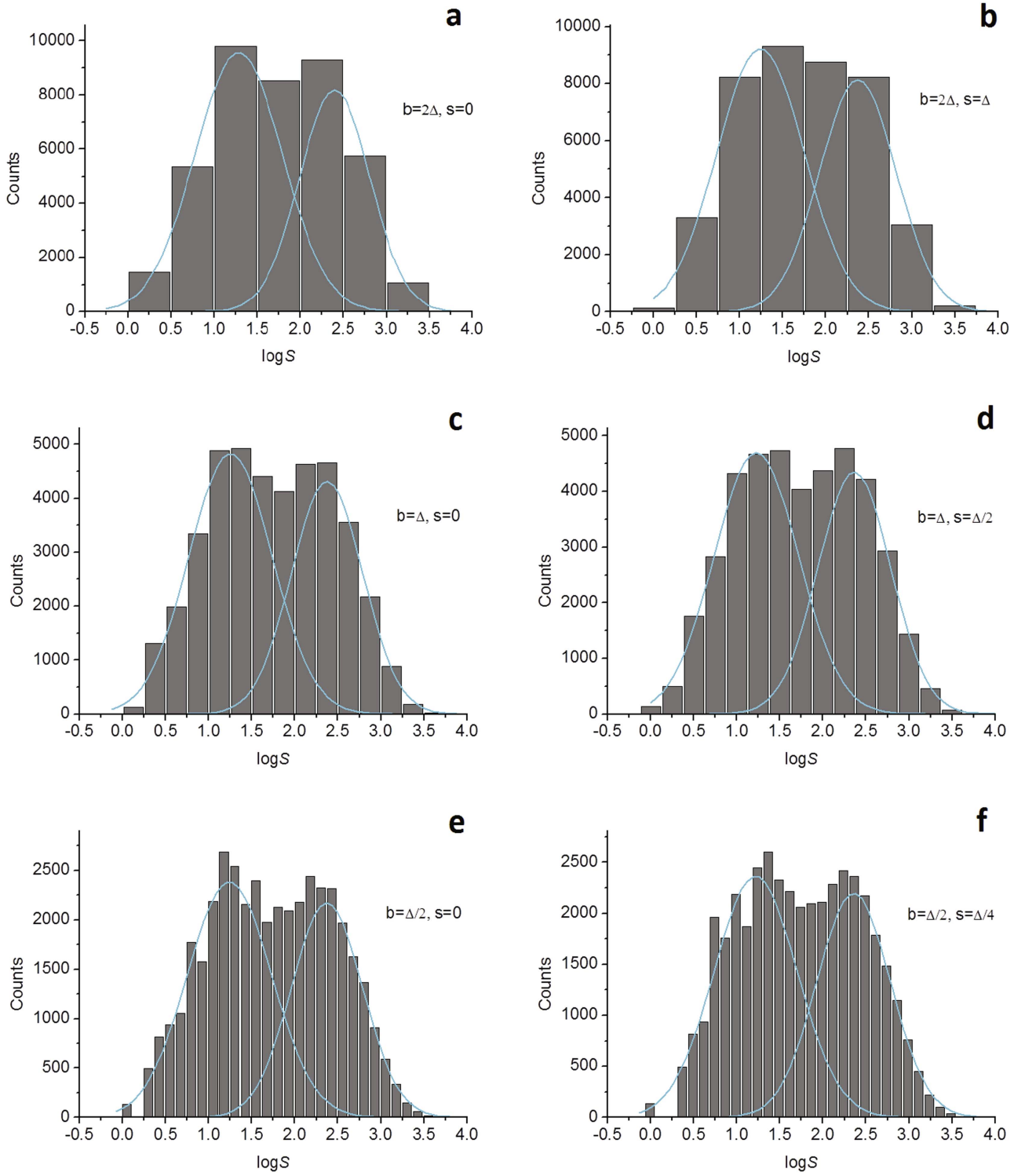

Figure 2. (a) Distribution of group areas (log S) from RGO data for different binning. Upper (a, b) and lower (e, f) panels show distributions with binning size double (half) compared to the binning size (Δ) used in Figure 1 (shown in panels c, d). Left column panels (a, c, and e) represent distributions with no shift in origin of the bins. The origin of the bins in distributions shown on the right (panels b, d, and f) are shifted by half their bin size. Blue solid lines indicate the Gaussian functions fitted to two separate components of the distribution.

observed PDFs of sunspot group areas for different cycles. The annualized mean of the "small area" component varies significantly from one solar cycle to the other. Thus, for example, between cycle 11 and cycle 15, the mean of distribution corresponding to the "small" groups shifts gradually from $\log S \approx 1.75$ (56 M.S.H.) to $\log S \approx 0.75$ (5.6 M.S.H.). The mean of the "large" sunspot group distribution also shifts to smaller areas from $\log S \approx 2.6$ (400 M.S.H.) in cycles 11–12 to $\log S \approx 2.3$ (200 M.S.H.) in cycle 13. However, between cycles 13 and 24, the mean position of this component does not change significantly.

Table 1
Mean, σ, and r of Fitted Bi-Gaussian Distributions

Bin size and Shift	x_L	σ_L	x_R	σ_R	r[a]	Ref.
$b = 2\Delta$, $s = 0$	1.288	0.511	2.402	0.406	0.999	Figure 2(a)
$b = 2\Delta$, $s = \Delta$	1.242	0.507	2.372	0.445	0.999	Figure 2(b)
$b = \Delta$, $s = 0$	1.254	0.486	2.377	0.414	0.998	Figure 2(c)
$b = \Delta$, $s = \Delta/2$	1.227	0.490	2.364	0.423	0.999	Figure 2(d)
$b = \Delta/2$, $s = 0$	1.241	0.489	2.372	0.414	0.991	Figure 2(e)
$b = \Delta/2$, $s = \Delta/4$	1.218	0.483	2.356	0.428	0.989	Figure 2(f)

Note.
[a] r–Pearson correlation coefficient between observed and fitted distributions.

3.2. Lifetime as a Separation Parameter

The lifetime of individual active regions may vary significantly depending on their level of activity. Nevertheless, there is a general correlation between size (area and total magnetic flux) and the lifetime of active regions ($T_{\rm life}$), with smaller groups disappearing faster than the larger groups (e.g., van Driel-Gesztelyi & Green 2015, and references therein). One can hypothesize that $T_{\rm life}$ can be used as an independent parameter to separate the two components contributing to the bimodal distribution of group areas. To determine the optimal threshold, which separates the two components, we divided our data set into two categories: those with $T_{\rm life} \leqslant m$(days) and with $T_{\rm life} > m$ (days). Next, we determined the best Gaussian fit to PDF of $\log S$ for each category using the following functional dependence:

$$G(x) = \sqrt{\frac{2}{\pi}}\frac{A_i}{W_i} e^{-\frac{2(x-C_i)^2}{W_i^2}}, \quad (3)$$

where A, C, and W are fitted parameters, and i designates the fitted parameters for small (S) and large (L) group areas.

For this test, we used $m = 3$, 4, 5, and 6 days. For each m, the fitted parameters were compared with the parameters of fitted Gaussians shown in Figure 1. We found that the best agreement between the Gaussian functions fitted to PDF in Figure 1(a) and the fitting based on the groups' lifetime threshold is achieved for $m = 5$ days (see, Figure 4). The coefficient of determination (Figure 4(e)) is highest for $m = 5$, and it indicates that about 99.67% of observed PDF is represented by this model.

Using the lifetime threshold allows us to deconvolve the 2D PDF of group areas shown in Figure 1(b) into two distinct categories: small groups with shorter lifetime (SSG, Figure 4(c)) and large groups with longer lifetime (LLG, Figure 4(f)). It is clear that the first category of sunspot groups shows long-term variations in its properties, while the properties of the second category of sunspot groups are more constant with time.

3.3. Changes with Phase of Solar Cycle

Recently, several authors reported that a relative fraction of small and large size sunspots may change from one cycle to the other (e.g., Lefèvre & Clette 2011; Nagovitsyn et al. 2012). This asymmetry is clearly visible in Figure 1(b) for the most recent cycles. For example, between year 2000 and 2005, the annualized distribution in size of active regions is centered at about $\log S \approx 2.2$, while for 2005–2010 period, mean $\log S \approx 1.5$. This visual appearance is further confirmed in Figure 5, which shows that the contribution of sunspot groups with longer lifetime/larger areas relative to the total number of sunspot groups also varies with the phase of cycle. On average, the fraction of LLG is smaller than 0.4 (40%) of all sunspot groups. Near the maximum of sunspot activity, the fraction of LLG increases. The largest LLG fraction of about 0.52 was observed in solar cycle 22. The smallest fraction of LLG was about 0.25 at the minimum of cycle 23. Interestingly, there appears to be no correlation between the amplitude of the solar cycle and fraction of LLGs. Thus, for example, although cycle 19 was the strongest by its amplitude, it had a smaller fraction of LLGs compared with cycles 14, 18, and 21–23 (Figure 5). In 8 out of 12 cycles (67%) the peak in LLG number occurred a few years after the peak in the total number of active regions. In three cycles, the LLG peak occurred earlier than the peak in the group number. Only in cycle 16 did the two peaks occur in the same year. In contrast, the minima in LLGs and the group number occurred in the same year for all cycles. A systematic shift between the maximum in LLGs and the group number could reflect the double-peaked nature of nearly all solar cycles (Gnevyshev 1967), when the activity (sunspot number) reaches the maximum, declines, and rises again to a second maximum. A dip between the two maxima, called "Gnevyshev gap," was interpreted as the presence of two waves of solar activity (e.g., Hathaway 2015). Georgieva (2011) suggested that the double maxima in the sunspot cycle may manifest the two surges of toroidal field, "one generated from the poloidal field advected

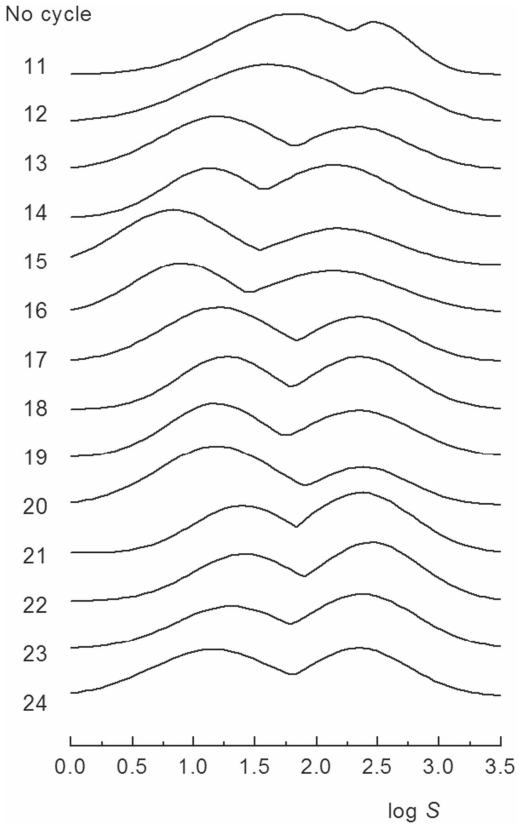

Figure 3. Bi-Gaussian function fitted to observed PDFs of group areas by a solar cycle. For display purposes, each fitted curve was normalized by its maximum amplitude, and shifted by a fixed value relative to neighboring cycles. Labels on the left side correspond to a solar cycle number.

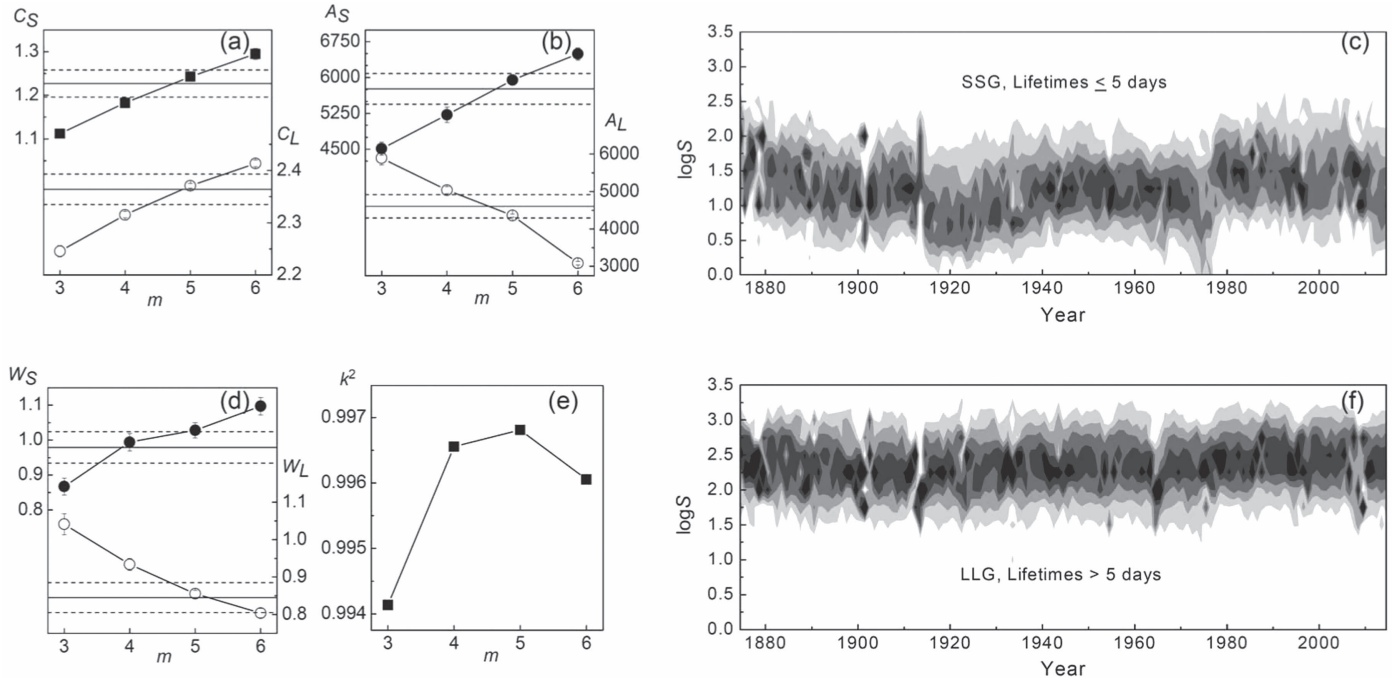

Figure 4. Two components of PDF log S (group area) separated by the group lifetime. (a) Fitted mean (A) of small (S, filled circles) and large (L, open circles) groups computed for different lifetime, m thresholds. Means of two Gaussians fitted to PDF in Figure 1(a) and their one standard deviations are shown as horizontal solid and dashed lines. (b) Same as panel (a) but for amplitude B of fitted Gaussians. (d) Same as panel (a) but for width W of fitted Gaussians. (e) The coefficient of determination of two Gaussian fits computed for different m. Panels (c) and (f) show resulting 2D annualized PDFs of group areas for groups with lifetime less than 5 days and those that persisted longer than 5 days.

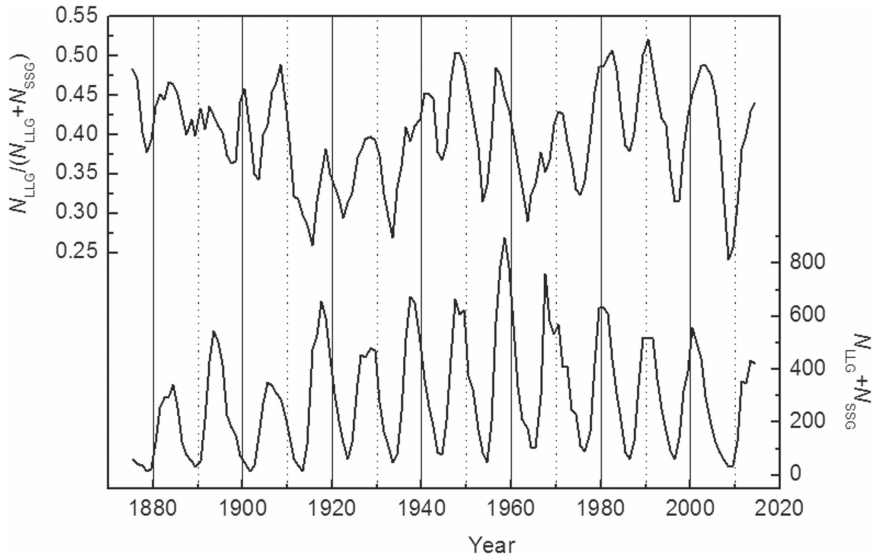

Figure 5. Annualized fraction of longer lifetime (large) sunspot groups (upper plot and the total number of groups as function of time. To simplify the comparison of two plots, vertical lines are plotted at 10 year intervals.

all the way on the surface to the poles, down to the tachocline and equatorward to sunspot latitudes, and another one generated from the poloidal field diffused at mid-latitudes from the surface to the tachocline and transformed there into toroidal field." Figure 1 in Georgieva (2011) provides a good graphical example of Gnevyshev gap in cycles 12–23. Visual comparison of Figure 5 with Figure 1 in Georgieva (2011) indicates that first the maxima (of solar cycles) coincide with the maxima in the total number of sunspot groups (lower plot in Figure 5), while the second maxima coincide with the maxima in LLG fraction (upper plot in Figure 5). For cycles that do not exhibit a clear Gnevyshev gap in the annual sunspot numbers, we see no temporal shift between the peaks in the group number and the relative LLG number. Large complexes of activity, which contribute to building up new polar field after its reversal, are formed at the declining phase of solar cycles, and the peak in LLGs may reflect the development of such complexes of activity.

Muñoz-Jaramillo et al. (2015b) deconvolved the distribution of areas of sunspot groups on two components: Weibull (small sunspots) and log-normal (large sunspots), and argued that properties of Weibull component do not significantly vary with

the level of solar activity. Our Figure 4(c), however, indicates that properties of SSGs clearly change with time. Indeed, logarithmic means and standard deviation (σ) computed for RGO data for three activity levels have similar properties: 1.76 ± 0.74 (low activity), 1.83 ± 0.74 (moderate), and 1.86 ± 0.72 (high). The reader should note that here we use natural logarithms, while Muñoz-Jaramillo et al. (2015b) employed common (or decadic) logarithms. For this test, we defined activity levels based on the total number (N_a) of groups per annum as following: $N_a \leqslant 100$, $300 \geqslant N_a \leqslant 400$, and $N_a \geqslant 600$. For comparison, logarithmic means and standard deviations computed for two different periods of solar activity cycles do show significant difference: 1.56 ± 0.78 (1915–1925) and 1.90 ± 0.74 (1950–1960). Thus, our results do not contradict previous findings about the independence of properties of distribution of small sunspots on the level of solar activity (Muñoz-Jaramillo et al. 2015b), but it appears that the contribution to different parts of that distribution may change from cycle to cycle.

4. DISCUSSION

Using a combined data set of sunspot group areas from the RGO (1874–1976), and the KMAS of the Central (Pulkovo) Astronomical Observatory (KMAS, 1977–2014), we study the distribution of sunspot groups by their area. Our results confirm the presence of two main components in the distribution, with one contribution peaking at about an area of a few tens of M.S.H. and the other at areas of about 300 M.S.H. Adopting a group's lifetime as a separating factor, we show that the two components can be reliably separated using 5 day lifetime as a threshold: small (in area) SSGs contribute mostly to one category, while LLGs form a different category. Annual 2D PDFs indicate that the peak of LLG distribution does not vary significantly from one cycle to the other. In contrast, the mean of SSG distribution shows significant long-term variations.

On a cycle-by-cycle basis, we see long-term variations in mean properties of SSGs, i.e., in some cycles, the mean of SSG contribution is smaller, but in others, it is larger. This might have some important consequences for the overall activity during each cycle. For example, taking into consideration that on average the flare productivity of an active region correlates with its total area (magnetic flux), one could expect that cycles with a large number of SSGs would have a lower level of flare activity compared with cycles, which exhibit a larger fraction of large sunspot groups. The fact that the LLG component does not significantly change over the last century, may also be taken as an argument against a possible development of an unusually large sunspot group ("superactive region"), which could produce a superflare, unless the process of the generation of sunspots changes dramatically from its present state. We also interpret the presence of long-term variations in statistical properties of SSG and the lack of those in the LLG component as a possible indication that SSG and LLG populations may be the result of separate dynamo processes. If SSG population was only the result of the fragmentation of larger groups, one would expect to see similar long-term variations in both populations. Furthermore, a systematic shift between the maxima of the solar cycles as represented by the annualized fraction of LLG and the total number of groups (SSG+LLG), may be seen as another indirect indication that SSG and LLG are produced differently irrespective of whether they have a single (spatially distributed) dynamo or independent dynamo mechanisms.

Y.A.N. acknowledges the partial support by the Russian Foundation for Basic Research (Project no. 16-02-00090), the Presidium of the Russian Academy of Sciences (Program no. 7), and the Council for support of leading scientific schools of the Russian Federation (Grant HIII-7241.2016.2). A.A.P. acknowledges the financial support by the Academy of Finland to the ReSoLVE Centre of Excellence (Project no. 272157). The National Solar Observatory is operated by AURA, Inc. under a cooperative agreement with the National Science Foundation. We thank the anonymous reviewer for his/her constructive comments, which led to the improvement of this paper.

Software: PowerBasic, ORIGIN, IDL.

REFERENCES

Cho, I.-H., Cho, K.-S., Bong, S.-C., et al. 2015, ApJ, 811, 49
Georgieva, K. 2011, ISRAA, 2011, 437838
Gmurman, V. E. 1968, Fundamentals of Probability Theory and Mathematical Statistics (1st ed.; New York: Elsevier)
Gnevyshev, M. N. 1967, SoPh, 1, 107
Godier, S., & Rozelot, J. P. 2001, SoPh, 199, 217
Hathaway, D. H. 2015, LRSP, 12, 4
Howard, R. 1984, ARA&A, 22, 131
Lefèvre, L., & Clette, F. 2011, A&A, 536, L11
Muñoz-Jaramillo, A., Senkpeil, R. R., Longcope, D. W., et al. 2015, ApJ, 804, 68
Muñoz-Jaramillo, A., Senkpeil, R. R., Windmueller, J. C., et al. 2015, ApJ, 800, 48
Nagovitsyn, Y. A., Pevtsov, A. A., & Livingston, W. C. 2012, ApJL, 758, L20
Penn, M. J., & Livingston, W. 2006, ApJL, 649, L45
Penn, M. J., & Livingston, W. 2011, in IAU Symp. 273, The Physics of Sun and Star Spots, ed. D. P. Choudhary & K. G. Strassmeier (Cambridge: Cambridge Univ. Press), 126
Pevtsov, A. A., Maleev, V. M., & Longcope, D. W. 2003, ApJ, 593, 1217
Pevtsov, A. A., Nagovitsyn, Y. A., Tlatov, A. G., & Rybak, A. L. 2011, ApJL, 742, L36
Press, W. H., Teukolsky, S. A., Vetterling, W. T., & Flannery, B. P. 1992, Numerical recipes in C. The art of scientific computing (2nd ed.; Cambridge: Cambridge Univ. Press)
Tlatov, A. G., Makarova, V. V., Skorbezh, N. N., & Muñoz-Jaramillo, A. 2016, "Kislovodsk Mountain Astronomical Station (KMAS) sunspot Group Data," Harvard Dataverse, V1
Tlatov, A. G., & Pevtsov, A. A. 2014, SoPh, 289, 1143
van Driel-Gesztelyi, L., & Green, L. M. 2015, LRSP, 12, 1
Ward, F. 1966, ApJ, 145, 416
Willis, D. M., Coffey, H. E., Henwood, R., et al. 2013, SoPh, 288, 117